CERN-INTC-2020-031 / INTC-P-532-ADD-1
13/05/2020

EUROPEAN ORGANIZATION FOR NUCLEAR RESEARCH

Addendum to IS652 experiment – ISOLDE and Neutron Time-of-Flight Committee

The peculiarities of reduction and doping of vanadium oxides probed by TDPAC spectroscopy at ISOLDE

May 13, 2020

A. W. Carbonari[1], R. N. Saxena[1], A. Burimova[1], L. F. D. Pereira[1], T. N. S. Sales[1], O. F. S. Leite Neto[1], F. A. Genezini[1], I. S. Ribeiro Junior[1], B. Bosch-Santos[2], E. L. Correa[2], G. A. Cabrera-Pasca[3], R. S. Freitas[4], D. Richard[5], J. Schell[6,7], J. G. M. Correia[6,8], D. C. Lupascu[7]

[1]*Instituto de Pesquisas Energéticas e Nucleares. IPEN, São Paulo, SP, Brazil*
[2]*Material Measurement Laboratory, NIST, Gaithersburg, MD 20899, USA*
[3]*Universidade Federal do Pará, Campus de Abaetetuba, Pará, Brazil*
[4]*Instituto de Física da Universidade de São Paulo (IFUSP), São Paulo, SP, Brazil*
[5]*Departamento de Física, Facultad de Ciencias Exactas, Universidad Nacional de La Plata, La Plata, Argentina*
[6]*EP Department, ISOLDE-CERN, CH-1211 Geneva 23, Switzerland*
[7]*Institute for Materials Science and Center for Nanointegration Duisburg-Essen (CENIDE), University of Duisburg-Essen, 45141 Essen, Germany*
[8]*Centro de Ciências e Tecnologias Nucleares (CCTN), IST, Universidade de Lisboa, Portugal*

Spokesperson: Anastasia Burimova anstburimova@gmail.com, Artur Wilson Carbonari carbonar@ipen.br, Juliana Schell juliana.schell@cern.ch
Contact person: Juliana Schell, João Guilherme Martins Correia guilherme.correia@cern.ch

Abstract: We propose a continuation of the study of intrinsic effects in vanadium oxides. The mechanism of temperature induced reduction in V_2O_5 is to be probed by TDPAC spectroscopy with ^{111m}Cd probes implanted at ISOLDE. We expect to extract information on the dynamics of oxygen vacancies and identify all the reduction products. In addition, a study of cadmium meta- and pyrovanadates is to be performed in order to elucidate the nature of Cd doping in V_2O_5. We intend to test the hypothesis that, even at low concentrations of the divalent metal, vanadate formation is favored and not substitutional doping.

Requested shifts: 6 shifts (split among two probe isotopes according to ISOLDE schedule)

1 Introduction and motivation

The current research plan may be considered as a continuation of IS652. Initially, a study of doping phenomenology in vanadium oxides was proposed. The project implementation, however, has lead to the development of an ancillary branch related to the reduction mechanisms in these materials.
The reduction of V_2O_5 is a complex process that has been approached by many groups and still is a matter of debate. For instance, the electron beam induced comproportional nucleation of V_6O_{13} and VO_2, where V_6O_{13} is the result of V_2O_5 layer shearing, or consecutive reduction of V_6O_{13} to VO_2 didn't gain evidence when temperature was used instead of electron beam to provoke oxygen desorption. In the latter case a direct $V_2O_5 \rightarrow VO_2$ conversion was identified [1–3].
The number of metastable phases, the capriciousness at changing external conditions and lack of accurate description of local behavior already resulted in severe misinterpretation of experimental outcomes for vanadium oxides [4–6]. Appropriate theoretical and experimental methods with strict control should, therefore, be exploited for these systems. Such precise local technique as TDPAC spectroscopy, allowing sub-nanoscale probing of atomic environments, appears as an excellent tool to elucidate temperature induced reduction mechanisms in V_2O_5. In this proposal we demonstrate the potential of the method and specify the challenges already faced.

Following the original line related to doping mechanisms in vanadium oxides, we intend to define the localization of the guest ions with the implementation of the current proposal. Particularly, we want to identify if the substitution of the host atoms, an occupation of intermediate positions or any other effect occurs and how these phenomena are affected by the synthesis conditions, structural peculiarities of the host, etc.
Doping is widely exploited as a means of application-oriented tuning of the material properties, and a common jargon usually exists in coupled research areas. For oxides the term itself is, in a great number of cases, used to indicate substitution at the atomic level. Moreover, when the guest concentration is small, conventional characterization methods may fail to show the formation of different phases, thus "confirming" the substitution. E. g. vanadates of different types are known, but not always noticed, to nucleate in attempts to dope V_2O_5 even at low concentrations [7–10]. For the ascription of the new or enhanced features this results in general confusion. Obviously, only unambiguous system characterization at the local level would allow establishing the desired control over its properties.
We propose a series of CdO–V_2O_5 systems, including meta- and pyrovanadates, CdV_2O_6 and CdV_2O_7 respectively, as a model for meticulous analysis of the doping mechanism in divanadium pentoxide. The issues to be addressed include, but are not limited to, (i) the concentration cap for Cd→V substitution; (ii) local environment of the dopant and (iii) the temperature induced structural transitions in vanadates.
Apart from purely fundamental interest, the introduced topic has strategic relevance. Previously, in IS652, we stressed on the applications of vanadium oxides in catalysis, for the production of chemical sensors and optoelectronic devices, electrochemical energy storage, etc. Meanwhile, at the industrial level, for the extraction of vanadium from raw

materials, the knowledge of physico-chemical properties of divalent vanadates is of great importance (see e.g. [11, 12]). To increase the extraction efficiency and to control the ecological impact, a deep understanding of the formation mechanism of vanadium-oxide-based compounds and their behavior under different conditions is crucial. This knowledge can be reached by addressing the model vanadate systems as suggested.

2 Objectives

As a result of the proposed work, we intend to (i) unambiguously classify cadmium doping of vanadium oxides and describe the effect of the dopant on the host in detail; (ii) fully characterize the structural transition in cadmium metavanadate at the local level; (iii) give new insights on the reduction mechanism of vanadium oxides.

3 Description of the proposed work

3.1 Route to achieve the proposed objectives

Up to now, our team has taken advantage of the two Cd runs at ISOLDE in 2018. Apart from ^{111m}Cd(^{111}Cd), ^{111}In probe generator was used at the home institution. The study is expected to benefit from the use of ^{111}Cd(^{117}In), complementing previous results and imitating an alternative doping scenario.
TDPAC spectroscopy continues to be the core technique of the project allowing insights into the structure, charge distribution symmetry and defects around the probe. The experience gained due to the previous activities would permit the fine-tuning of our TDPAC session at ISOLDE. More specific examples follow:

- a refined procedure for mapping the reduction mechanism: increase of the surface area in order to provoke oxygen diffusion at higher rate. This may be reached by exploiting nanosize samples (to be prepaired for this purpose);
- a series of TDPAC measurements of synthesized pyro- and ortovanadates in variable conditions, as well as vanadium oxides of "intermediate stoichiometries" (e. g. V_6O_{13});
- more efficient protocols of post-implantation treatment tested for vanadate samples at the home institution;
- measurements in intermediate temperature ranges;
- TDPAC study of acquired vanadium oxide high purity standards.

3.2 Preparation and characterization of samples at home institutions

Through the previous stages of the project, the sufficiency of Hyperfine Interactions Laboratory (HIL, IPEN) infrastructure and staff competence to prepare samples of adequate

quality was evidenced.
A number of methods was exploited including sol-gel, co-precipitation and hydrothermal synthesis, resulting in the preparation of vanadium oxides of different stoichiometries, pyro- and metavanadates of cadmium. We here emphasize the use of different precursors as well: V_2O_5 and metallic vanadium. The quality control was and is to be performed at IPEN, principally via X-ray diffractometry (XRD) and electron microscopy.
A Scanning Probe Microscopy/Optical platform recently acquired by IPEN should allow access to a series of tools including Raman spectroscopy (conventional and tip-enhanced) and atomic force, scanning near-field optical, tunneling microscopies. Those may be of special interest for a detailed characterization of nanoscale vanadia-based samples.

3.3 DFT simulations at home institutions

We exploit first-principles calculations, using full-potential augmented plane waves plus local orbital method (FP-APW+lo) based on the DFT to simulate the doping in the host oxides to interpret the experimental hyperfine interactions results. All-electron *ab initio* electronic structure calculations in the framework of the density functional theory (DFT) have shown to be effective for studying structural deformations, localization and charge states of defect centers and impurities, the character of the impurity levels, etc; so good approximations may be obtained for the hyperfine parameters [13–16].
The simulations related to this project are already running and have reasonable compatibility with experiments so far. Several trials with ELK code were performed to probe the electric field gradient (EFG) at the sites of monoclinic and rutile phases of VO_2. For β-CdV_2O_6 a number of approaches has been tested, the results are summarized in Section 3.5.

3.4 PAC Spectroscopy technique and methodology justification

The method is based on the conservation of angular momentum between the spin direction of the γ-emitter probe nucleus and the direction of the γ emission pattern. The hyperfine interaction consists of the coupling of the total angular momentum ($\vec{J}$) of the electrons with the nucleus spin ($\vec{I}$). When the probe nucleus is inserted into a material, the hyperfine interaction induces a time variation of this emission pattern and its measurement in a plane at different angles permits obtaining the EFG and/or the magnetic hyperfine field. Combined electrical plus magnetic hyperfine interactions can also be measured.
The number of radioactive nuclei, which are necessary to perform experiments, is generally less than 10^{12}, at very low concentrations, generally, in the range between 0.01% and ppm. This number of atoms is still enough to produce an observable modulation of the decay curve, described by the anisotropy ratio, $R(t)$. A fit to this curve allows identifying multiple fractions of probe atoms interacting with certain local environments. Phenomena related to the observation of lattice sites, defects, orbital ordering, electronic polarization, all being investigated as a function of parameters like temperature, electric field, and pressure are examples of the potentiality of the PAC technique. PAC is, therefore, suitable to a precise and detailed characterization of nanoscopic materials mainly because it can obtain information on different regions inside the sample. As mentioned previously, the

method is complemented by first-principles calculations and this complementarity has been used with success by our team [13–17].

3.5 Report: Resume of our earlier findings

The quality control over commercial V_2O_5 and synthesized at HIL samples was realized via XRD. TDPAC measurements with ^{111}In probe generator were performed at HIL under a variety of conditions and selected results are shown in Figure 1. The probes were introduced to the samples via wet impregnation and directly at synthesis, and no significant difference in the corresponding results was observed.

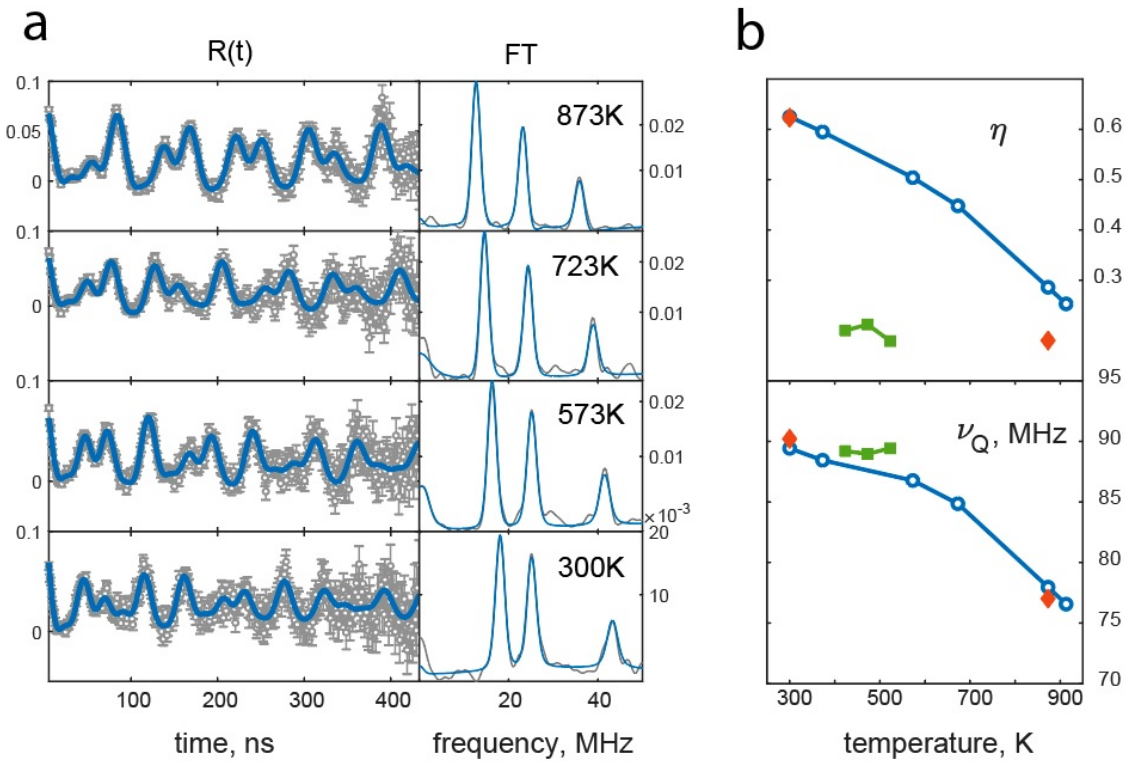

Figure 1: TDPAC $R(t)$ spectra with their Fourier transforms recorded at different temperatures of (initially pure) V_2O_5 (a); corresponding quadrupole coupling constant (ν_Q) and asymmetry parameter (η) evolution at cooling (b). ♦ indicates the results of measurements at ISOLDE with ^{111m}Cd, ■ represents the results obtained by Naicker *et al.* [18, 19]

Importantly, a good probe diffusion (or relaxation) suitable for TDPAC measurements was attained only at 773–823 K in vacuum. The attempts of sample annealing in O_2 and air weren't successful. The scenario repeated itself for ^{111m}Cd probe parent at ISOLDE. One may note the corresponding low values of asymmetry η obtained at high temperature in the environment with continuous evacuation. All in all, it indicates that the relaxation of Cd ions in V_2O_5 only occurs upon oxygen diffusion and a consequent reduction of the host. This assumption is further supported by our post-annealing XRD data that revealed monoclinic VO_2 and V_6O_{13} next to V_2O_5.

Furthermore, hyperfine parameters thus obtained have general resemblance with the previous ^{51}V Nuclear Magnetic Resonance (NMR) spectroscopy results for (assigned) monoclinic VO_2 [20–23] and, to a lower degree to those of V_6O_{13} [24]. At the same time, NMR studies of V_2O_5, somewhat counterintuitively, revealed a relatively symmetric environment of V [25–27].

We therefore assume that the observed site unlikely represents the straightforward substitution of V^{5+} of the pentoxide matrix by the probe. However, more information is needed to unambiguously attribute it to the occupation of a specific site in V_6O_{13} or (monoclinic/tetragonal)-VO_2.

The results summarized in Table 1 demonstrate the change in hyperfine parameters for higher Cd concentrations. Our study and previous findings for pyro- and metavanadates of cadmium indicate the formation of similar phases in the synthesized samples even when slightly doped (see Figure 2).

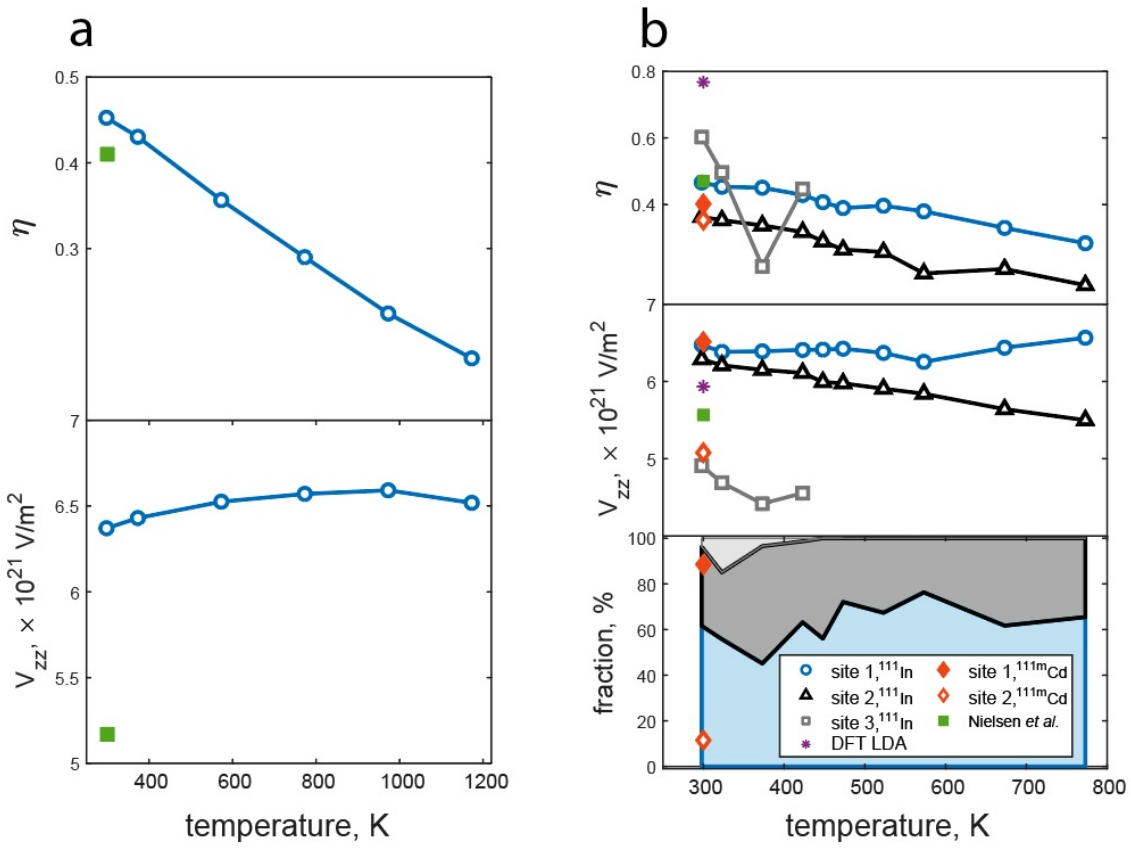

Figure 2: Evolution of hyperfine parameters with temperature obtained for (initially) $Cd_2V_2O_7$ (a); same for CdV_2O_6 (b). ■ refer to previous findings by Nielsen *et al.* for pyro- (a) and β-metavanadate (b) [28]. DFT (LDA) results for Cd site in β-CdV_2O_6 are marked with ∗.

Again, although the general picture is relatively clear and the doping is unlikely substitutional, it is not yet possible to assign (even the narrow distributed) frequencies to a particular structure. First, Cd nearest neighbour environments of α and β phases of metavanadate are similar. Second, they appear highly symmetric. Third, although a transition to the α phase should occur at ∼473 K, it was shown to stabilize at lower tem-

peratures as well. And, finally, temperature and pressure conditions allow the coexistance of pyro-, metavanadates and V_2O_5 [29]. Besides, we still do not exclude Cd probe at the distorted V site in vanadates.

Table 1: EFG characterization obtained for nCdO·V_2O_5 mixtures at IPEN (measurements with ^{111}In $\rightarrow$ ^{111}Cd) and ISOLDE (measurements with ^{111m}Cd $\rightarrow$ ^{111}Cd). The work on the proposed project implies data completion

Parent isotope	**Cd frac.**	**site 1**			**site 2**			**site 3**		
		ν_Q, MHz	η	δ, %	ν_Q, MHz	η	δ, %	ν_Q, MHz	η	δ, %
	$\leqslant$0.01	118.7	1	7.3	109.3	0.36	6.24	138.9	0.29	55.0
^{111}In	0.05	117.9	0.95	2.65	108.6	0.38	1.19			
	0.1	116.9	0.94	0.93	106.6	0.44	22.17			
	$n=1$	113.7	0.47	8.22	110.4	0.36	5.20	86.2	0.60	0.0
	$n=2$	111.9	0.45	5.21						
	$\leqslant$0.01	118.4	0.29	63.8	95.6	0.6	4.85			
^{111m}Cd	0.05	119.6	0.96	2.34						
	0.1	117.3	0.96	2.45	110.1	0.33	2.88			
	$n=1$	114.4	0.40	3.16	89.2	0.35	10.28			
	$n=2$	–	–	–						

***Ab initio* simulations**

The results for main hyperfine parameters of β-CdV_2O_6 obtained with DFT exploiting WIEN2k are summarized in Table 2, were transferred to Figure 2b, and remain in good agreement with experimental data. The EFG values obtained using the Elk code for undoped vanadium dioxide in monoclinic and rutile phase are ∼40% different from experiment and thus were not presented here.

Table 2: The results of DFT simulations for β-CdV_2O_6

Method	Site	$\lvert V_{zz}\rvert$, V/m^2	η
PBE	**Cd**	6.00173	0.93851
	V	4.33435	0.66119
WC	**Cd**	5.93722	0.89003
	V	4.73933	0.75448
LDA	**Cd**	5.93436	0.7679
	V	5.08049	0.86838

To fully complement the experiments, DFT study of α-CdV_2O_6, $Cd_2V_2O_7$ and vanadia with dispersed dopants are to be performed with WIEN2k. We entend to continue adjusting the Elk simulations, since the code has shown good performance with a trial TiO_2 system (somewhat similar to VO_2).

Summary of requested shifts: We estimate the total amount of ISOLDE beam time needed to implement the proposal as 6 shifts distributed according to Table 3.

Table 3: Beam time request for PAC studies

Required isotope	Implanted beam	Probe element	Type of exp.	Approx. Intensity [at/μC]	Target/Ion source	Required atoms per sample	Comments	# of shifts
^{111m}Cd (48m)	^{111}Cd	^{111}Cd	$\gamma-\gamma$ PAC	10^8	Sn target; VD 5 ion source	2×10^{10}		4
^{117}Cd (2.49h)	^{117}Ag	^{117}In	$\gamma-\gamma$ PAC	10^8	UC target; RILIS (Ag) ion source	5×10^{10}		2
Total # of requested shifts								**6**

References

[1] J. Haber, M. Witko, and R. Tokarz. Vanadium pentoxide i. structures and properties. *Applied Catalysis A: General*, 157:3–22, 1997. doi: 10.1016/S0926-860X(97)00017-3.

[2] D. S. Su, M. Wieske, E. Beckmann, A. Blume, G. Mestl, and R. Schlögl. Electron beam induced reduction of V_2O_5 studied by analytical electron microscopy. *Catalysis Letters*, 75(1–2):81–86, 2001. doi: 10.1023/A:1016754922933.

[3] D. S. Su and R. Schlögl. Thermal decomposition of divanadium pentoxide V_2O_5: Towards a nanocrystalline V_2O_3 phase. *Catalysis Letters*, 83(3):115–119, 2002. doi: 10.1023/A:1021042232178.

[4] A. Pergament, G. Stefanovich, and V. Andreeev. Comment on "metal-insulator transition without structural phase transition in V_2O_5 film". *Appl. Phys. Lett.*, 102 (176101):1, 2013. doi: 10.1063/1.4804203.

[5] M. Kang, I. Kim, S. W. Kim, J.-W. Ryu, and H. Y. Park. Metal-insulator transition without structural phase transition in V_2O_5 film. *Appl. Phys. Lett.*, 98(131907):1–3, 2011. doi: 10.1063/1.3571557.

[6] R.-P. Blum, H. Niehus, C. Hucho, R. Fortrie, M. V. Ganduglia-Pirovano, J. Sauer, S. Shaikhutdinov, and H.-J. Freund. Surface metal-insulator transition on a vanadium pentoxide (001) single crystal. *Phys. Rev. Lett.*, 99(226103):1–4, 2007. doi: 10.1103/PhysRevLett.99.226103.

[7] R. Suresh, K. Giribabu, R. Manigandan, S. Munusamy, S. Praveen Kumar, S. Muthamizh, A. Stephen, and V. Narayanan. Doping of Co into V_2O_5 nanoparticles enhances photodegradation of methylene blue. *Journal of Alloys and Compounds*, 598:151–160, 2014. doi: 10.1016/j.jallcom.2014.02.041.

[8] D. Zhu, H. Liu, L. Lv, Y. D. Yao, and W. Z. Yang. Hollow microspheres of V_2O_5 and Cu-doped V_2O_5 as cathode materials for lithium-ion batteries. *Scripta Materialia*, 59:642–645, 2008. doi: 10.1016/j.scriptamat.2008.05.020.

[9] H. Zeng, D. Liu, Y. Zhang, K. A. See, Y.-S. Jun, G. Wu, J. A. Gerbec, X. Ji, and G. D. Stucky. Nanostructured Mn-doped V_2O_5 cathode material fabricated from layered vanadium jarosite. *Chem. Mater.*, 27(21):7331–7336, 2015. doi: 10.1021/acs.chemmater.5b02840.

[10] C. Xiong, A. E. Aliev, B. Gnade, and K. J. Balkus Jr. Fabrication of silver vanadium oxide and V_2O_5 nanowires for electrochromics. *ACS Nano*, 2(2):293–301, 2008. doi: 10.1021/nn700261c.

[11] T. K. Mukherjee and C. K. Gupta. Extraction of vanadium from an industrial waste. *High Temperature Materials and Processes*, 11(1–4):189–206, 1993. doi: 10.1515/HTMP.1993.11.1-4.189.

[12] H.-Y. Li, K. Wang, W.-H. Hua, Z. Yang, W. Zhou, and B. Xie. Selective leaching of vanadium in calcification-roasted vanadium slag by ammonium carbonate. *Hydrometallurgy*, 160:18–25, 2016. doi: 10.1016/j.hydromet.2015.11.014.

[13] D. Richard et al. Electronic and structural properties, and hyperfine interactions at Sc sites in the semiconductor Sc_2O_3: TDPAC and ab initio study. *Phys. Rev. B*, 82 (035206):1–9, 2010. doi: 10.1103/PhysRevB.82.035206.

[14] D. Richard, L. A. Errico, and M. Rentería. Electronic, structural, and hyperfine properties of pure and Cd-doped hexagonal La_2O_3 semiconductor. *Comp. Mater. Sci.*, 102:119–125, 2015. doi: 10.1016/j.commatsci.2015.02.023.

[15] D. Richard, M. Rentería, and A. W. Carbonari. Substitutional Ta-doping in Y_2O_3 semiconductor by sol-gel synthesis: experimental and theoretical studies. *Semicond. Sci. Technol.*, 32(085010):1–11, 2017. doi: 10.1088/1361-6641/aa7a74.

[16] C. Sena, M. S. Costa, E. L. Mu noza, G. A. Cabrera-Pasca, L. F. D. Pereira, J. Mestnik-Filho, A. W. Carbonari, and J. A. H. Coaquira. Charge distribution and hyperfine interactions in the vicinity of impurity sites in In_2O_3 doped with Fe, Co, and Ni. *Journal of Magnetism and Magnetic Materials*, 387:165–178, 2015. doi: 10.1016/j.jmmm.2015.03.092.

[17] J. Schell, D. C. Lupascu, A. W. Carbonari, et al. Cd and In-doping in thin film SnO_2. *J. Appl. Phys.*, 121(195303):1–5, 2017. doi: 10.1063/1.4983669.

[18] V. Naicker, A. Bartos, K. P. Lieb, M. Uhrmacher, T. Wenzel, and D. Wiarda. The electric field gradient at ^{111}Cd in vanadium oxides. *Hyperfine Interactions*, 80:965–970, 1993. doi: 10.1007/BF00567448.

[19] V. V. Naicker. *A study of the vanadium oxide bronze θ-VOB, and vanadium oxides V_2O_5 and VO_2, using hyperfine interaction techniques.* PhD thesis, University of Durban-Westville, 1 1999.

[20] J. M. Reyes, S. L. Segel, and M. Sayer. An nmr analysis of transitions in VO_2:Al. *Journal of Solid State Chemistry*, 12:298–302, 1975. doi: 10.1016/0022-4596(75)90329-1.

[21] G. F. Lynch, S. L. Segel, and M. Sayer. Nuclear magnetic resonance study of polycrystalline VO_2. *Journal of Magnetic Resonance*, 15(1):8–18, 1974. doi: 10.1016/0022-2364(74)90169-3.

[22] J. M. Reyes, S. L. Segel, and M. Sayer. An nmr study of low temperature phase of vanadium dioxide. *Low Temp. Phys.*, 26(2):197–203, 2000.

[23] U. Gro Nielsen, J. Skibsted, and H. J. Jakobsen. β-VO_2 – a V(IV) or a mixed-valence V(III)–V(V) oxide – studied by ^{51}v MAS NMR spectroscopy. *Chemical Physics Letters*, 356:73–78, 2002. doi: 10.1016/S0009-2614(02)00327-5.

[24] M. Itoh, H. Yasuoka, Y. Ueda, and K. Kosuge. NMR study of microscopic magnetic properties of V_6O_{13}. *J. Phys. Soc. Jpn.*, 53:1847–1856, 1984. doi: 10.1143/JPSJ.53.1847.

[25] H. Nagasawa, S. K. Takeshita, and Y. Tomono. Nuclear quadrupole moment of vanadium. *Journal of the Physical Society of Japan*, 19:764–765, 1964. doi: 10.1143/JPSJ.19.764.

[26] S. D. Gornostansky and C. V. Stager. Nuclear magnetic resonance study of V_2O_5. *The Journal of Chemical Physics*, 46:4959–4962, 1967. doi: 10.1063/1.1840660.

[27] V. Saraswati. Quadrupole interactions in vanadates. *Journal of the Physical Society of Japan*, 23(4):761–765, 1961. doi: 10.1143/JPSJ.23.761.

[28] U. G. Nielsen, H. J. Jakobsen, and J. Skibsted. Characterization of divalent metal metavanadates by ^{51}V magic-angle spinning NMR spectroscopy of the central and satellite transitions. *Inorg. Chem.*, 39:2135–2145, 2000. doi: 10.1021/ic991243z.

[29] M. Bosacka and A. Blonska-Tabero. Reinvestigation of system CdO-V_2O_5 in the solid state. *J Therm Anal Calorim*, 93:811–815, 2008. doi: 10.1007/s10973-008-9303-9.

Appendix

DESCRIPTION OF THE PROPOSED EXPERIMENT

The experimental setup comprises: (*name the fixed-ISOLDE installations, as well as flexible elements of the experiment*)

Part of the	Availability	Design and manufacturing
SSP-GLM chamber, SSP-GHM chamber	☒ Existing	☒ To be used without any modification
Existing equipment on the solid state labs in building 508-r-002, r-004 and r-008	☒ Existing	☐ To be used without any modification ☐ To be modified
	☐ New	☐ Standard equipment supplied by a manufacturer ☐ CERN/collaboration responsible for the design and/or manufacturing
[Part 2 of experiment/ equipment]	☐ Existing	☐ To be used without any modification ☐ To be modified
	☐ New	☐ Standard equipment supplied by a manufacturer ☐ CERN/collaboration responsible for the design and/or manufacturing
[insert lines if needed]		

HAZARDS GENERATED BY THE EXPERIMENT (if using fixed installation:) Hazards named in the document relevant for the fixed SSP-GLM chamber and building 508-r-002, r-004 and r-008 installations. Every experiment has its one written procedure file discussed with Radio Protection services, before every beam time.

Additional hazards:

Hazards	[Part 1 of experiment/ equipment]	[Part 2 of experiment/ equipment]	[Part 3 of experiment/ equipment]
Thermodynamic and fluidic			
Pressure	[pressure][Bar], [volume][l]	Vacuum	
Vacuum	10^{-6} mbar at SSP chamber 10 during collections	10^{-5} mbar	
Temperature	[temperature] [K]	Room temperature – 913 K	
Heat transfer			
Thermal properties of materials			
Cryogenic fluid	[fluid], [pressure][Bar], [volume][l]		
Electrical and electromagnetic			

Electricity	[voltage] [V], [current][A]		
Static electricity			
Magnetic field	[magnetic field] [T]		
Batteries	□		
Capacitors	□		
Ionizing radiation			
Target material [material]			
Beam particle type (e, p, ions, etc)	^{111m}Cd, ^{117}In		
Beam intensity			
Beam energy	50 keV		
Cooling liquids	[liquid]		
Gases	[gas]		
Calibration sources:	□		
• Open source	□		
• Sealed source	□ [ISO standard]		
• Isotope			
• Activity			
Use of activated material:			
• Description	□ Removal from chamber, transport to TD-PAC laboratory 508-r-002 in standard Pb castle shielding. Placed in PAC machine at 508-r-008 for measurement.		
• Dose rate on contact and in 10 cm distance	Max. 0.3 μSv/h (Nucleonica gamma dose rate)		
• Isotope	^{111m}Cd, ^{117}In		
• Activity	Max 6 MBq per sample		
Non-ionizing radiation			
Laser			
UV light			
Microwaves (300MHz-30 GHz)			
Radiofrequency (1-300 MHz)			
Chemical			
Toxic	[chemical agent], [quantity]	V_2O_5, V_6O_{13}, VO_2, $Cd_2V_2O_7$, CdV_2O_6	
Harmful	[chem. agent], [quant.]	V_2O_5, V_6O_{13}, VO_2, $Cd_2V_2O_7$, CdV_2O_6	

CMR (carcinogens, mutagens and substances toxic to reproduction)	[chem. agent], [quant.]		
Corrosive	[chem. agent], [quant.]		
Irritant	[chem. agent], [quant.]		
Flammable	[chem. agent], [quant.]		
Oxidizing	[chem. agent], [quant.]		
Explosiveness	[chem. agent], [quant.]		
Asphyxiant	[chem. agent], [quant.]		
Dangerous for the environment	[chem. agent], [quant.]	V_2O_5, V_6O_{13}, VO_2, $Cd_2V_2O_7$, CdV_2O_6	
Mechanical			
Physical impact or mechanical energy (moving parts)	[location]		
Mechanical properties (Sharp, rough, slippery)	[location]		
Vibration	[location]		
Vehicles and Means of Transport	[location]		
Noise			
Frequency	[frequency],[Hz]		
Intensity			
Physical			
Confined spaces	[location]		
High workplaces	[location]		
Access to high workplaces	[location]		
Obstructions in passageways	[location]		
Manual handling	[location]		
Poor ergonomics	[location]		

Hazard identification:

Average electrical power requirements (excluding fixed ISOLDE-installation mentioned above): [make a rough estimate of the total power consumption of the additional equipment used in the experiment]